

Human remains from Qareh Tepe, Iran, 2017-2018

Joanna Trębicka¹, Elham Farnam², Mostafa Dehpehlavan³,
Zahra Alinezhad², Arkadiusz Soltysiak^{*4}

¹ Antiquity of Southeastern Europe Research Centre, University of Warsaw,
Krakowskie Przedmieście 32, 00-927 Warszawa, Poland

² University of Tehran, Enghelab St., 14174-14418, Tehran, Iran

³ Institute of Archaeology, University of Tehran,
No. 13, Poorsina St., Qods St., Enghelab St., 14176-53911, Tehran, Iran

⁴ Department of Bioarchaeology, Institute of Archaeology, University of Warsaw,
Krakowskie Przedmieście 26/28, 00-927 Warsaw, Poland
email: a.soltysiak@uw.edu.pl (corresponding author)

Qareh Tepe (35°49'00''N, 49°57'08''E) is located in the NW part of the Iranian Central Plateau, 7km north of the small town of Sagzabad, in the Buein Zahra district. The Qazvin Plain, which surrounds the site, extends along the Alborz Mountains in this area for c. 60km. Composed of a series of alluvial fans, the Qazvin Plain provides a suitable place both for farming and animal husbandry. The southern part of the plain is provided with water by the Hajee Arab alluvial fan, with the village of Sagzabad at its top. Excavations of settlement and residential structures at Qareh Tepe were conducted in 2014–2015. During the survey aimed at defining the limits of Qareh Tepe, which was conducted in May 2016, a cemetery dated to the Iron Age II and III was found in the eastern part of the site.

Excavations at the newly discovered cemetery were initiated in 2017, in order to establish an accurate chronology of the graves and to increase knowledge about the burial practices and cultural patterns in the region. A new 10×20m trench (No. 12) was opened 180 meters north-east from the main site (**Figure 1**). Here the archaeologists discovered a multi-layer cemetery with the uppermost burial context found at a depth of 128cm (context 12016) and the deepest over two metres below (355cm; context 12048). Most of the documented graves were so-called chest or mudbrick four-sidewall graves. The majority of graves were multiple interment collective burials (contexts 12021, 12030, 12033, 12038, 12040 and 12047), with only one grave (context 12035) containing a single skeleton. Human remains were usually either partially or completely disarticulated, although occasionally preserved anatomical order was noted (context 12038).

In the majority of graves, the dead were buried with small ruminants, such as ovicaprids. Furthermore, in all burials various offerings were documented, such as gray, buff and red wares, bronze arrowheads and various metal ornaments (iron, bronze,

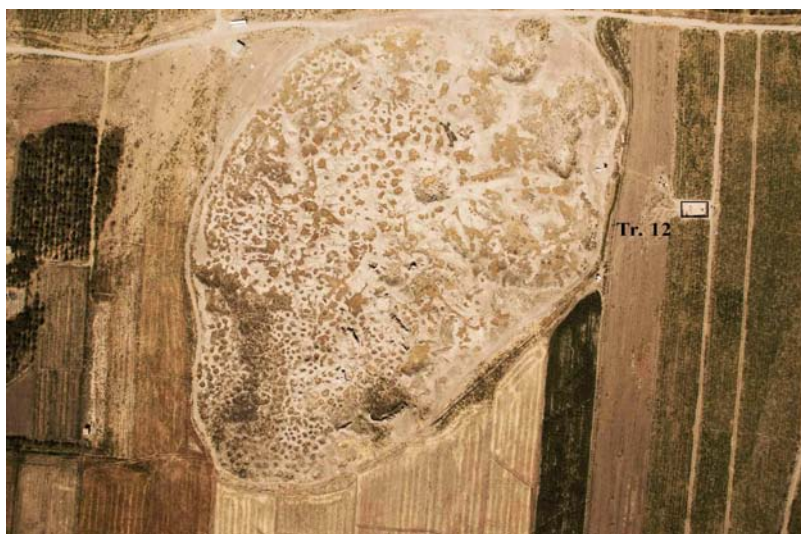


Figure 1. Location of trench 12 at Qareh Tepe.

shell, agate, limestone, glass paste). In one grave (context 12033) many cylinder seals were documented, which may indicate a high social status of the residents of Qareh Tepe. According to the cultural material, the relative chronology of layers 1 to 5 (excavated in 2017 and 2018) covers the Iron Age II and III (1100–550 BC). Two radiocarbon dates corroborated this dating: context 12047A dated to 1050–895 cal. BC (Poz-114528) and context 12035 dated to 924–812 cal. BC (Poz-114529).

Osteological analyses of the human remains from Qareh Tepe were conducted according to the protocols proposed by Brickley and McKinley (2004). The sex of adult individuals was assessed based on dimorphic morphologies of the pelvis (Phenice 1969; Buikstra & Ubelaker 1994) and skull (Acsádi & Nemeskéri 1970; Buikstra & Ubelaker 1994). The age-at-death of subadults was based on development and eruption of teeth (AlQahtani et al. 2010), as well as the diaphyseal lengths and epiphysis fusion status (Scheuer et al. 2010). In the case of adult individuals, ageing was based on morphological changes of the pubic symphysis (Brooks & Suchey 1990) and auricular surface (Buckberry & Chamberlain 2002). Stress markers, such as *cribra orbitalia* and porotic hyperostosis, were scored using the protocol presented by Steckel et al. (2006). Pathologies, including trauma and degenerative joint disease, were described based on the protocol of Waldron (2009), while dental caries were scored according to Hillson (2001).

Human remains were retrieved from 13 graves and four other contexts (12003, 12010, 12014 and 12027) that contained single human elements, accompanied by ashes and cultural waste materials. In most of the graves, human remains of more than

Table 1. Basic characteristics of human remains from Qareh Tepe.
CO – *cribra orbitalia*; PH – porotic hyperostosis.

Tag	Sex	Age-at-death	Caries	CO	PH	Completeness
12003	?	adult				fragmented temporal bone
12010A	?	adult	0/2			a few elements
12010B	–	1–3	0/1			deciduous canine
12014A	?	adult				a few elements
12014B	–	7–14				finger segment
12016	M**	senile	0/9	0	0	very incomplete
12018A	F**	mature	3/15	0	0	cranial vault & mandible
12018B	F**	adult	0/5	0	0	cranium
12018C	–	neonate				fairly complete, no legs
12018D	–	infant		0		fragments from upper skeleton
12018E	–	4		0		incomplete
12018F	M	adult				multiple bone assemblage
12018G	F**	adult				multiple bone assemblage
12021A	M**	adult	0/12			incomplete
12021B	?	adult	0/6			fragmented maxilla
12027	–	2–7			1*	cranial fragments
12030A	F	50–59	2/25	0	0	fairly complete
12030B	–	c. 15	0/28	0	0	cranium & mandible + mixed bones
12030C	M*	45–49*				incomplete postcranial skeleton
12039D	?	adult				foot bones
12033A	–	neonate				partially preserved
12033B	F	40–44	2/14	0	0	fairly complete
12033C	F	25–29	2/5	0	0	fairly complete
12033D	?	adult	0/15			mandible + mixed bones
12033E	?	adult				left 4 th metatarsal
12035	M	30–35	2/32	0	0	fairly complete
12036A	–	12–15	0/2			partially preserved
12036B	–	infant				multiple bone assemblage
12038A	F	40–50	1/15	0	0	almost complete
12038B	–	6		1	0	fairly complete
12038C	M	adult				incomplete
12038D	–	infant				left talus
12040	–	2–7				left lower extremity
12044	–	1.75		0		partially preserved
12047A	M	40–50	0/11	0	0	cranium + mixed bones
12047B	?	18–25	1/9			mandible + mixed bones
12047C	–	7–15				multiple bone assemblage
12047D	M*	adult	0/5			cranial vault + mixed bones
12047E	?	adult	0/16			mandible + mixed bones
12048A	?	adult				a few elements
12048B	–	7–15				lumbar vertebra



Figure 2. Coalition of the right talus and calcaneus of a male individual (12030C; 45–49* years old). Scale bar 1cm.

one individual were commingled, however in many cases it was possible to identify bones belonging to a single individual. The total minimum number of individuals is 41 (Table 1), including 8 males, 7 females, 10 adults of unknown sex, 5 children 8–15 years old, 4 children 2–7 years old, as well as 7 neonates and infants. Such age-at-death distribution roughly corresponds to an attritional cemetery and in this respect, the cemetery at Qareh Tepe differs from many other Iron Age cemeteries where subadult remains are under-represented (Sołtysiak et al. 2017; Hosseinzadeh et al. 2018; Sołtysiak et al. 2018; Szymczak et al. 2018).

The human remains from Qareh Tepe were very well preserved, as they were protected by dense clay soil and thick layers of alluvial deposit. The good state of preservation enabled detailed analysis of various pathologies that provided interesting information about the quality of life of the studied population.

Dental caries is an infectious disease, caused by biofilm bacteria (Waldron 2009). Their development is a multi-factorial process (Fejerskov 2004), but the abundance of fermentable sugars in a diet appears to be the crucial element (Hillson 1996). Among the analyzed human remains from Qareh Tepe, the dentition of 17 individuals was preserved, excluding a single tooth from non-burial context 12010. Carious lesions were observed in seven individuals, including five females, one male and one young adult of unknown sex. Although cavities were present in tooth enamel of one third of the individuals with preserved dentition, the frequency of disease was relatively low considering that caries were documented only in 13 out of 226 teeth (5.8%).



Figure 3. Two completely healed sharp force trauma lesions on the left parietal bone of a male individual (12035; 30–35 years old).

Cribra orbitalia (CO) and porotic hyperostosis (PH) are stress markers that develop in response to different environmental factors, such as malnutrition or infections (Walker et al. 2009; McIlvaine 2015). At Qareh Tepe, both CO and PH were infrequent and diagnosed only for subadults. In the group of 13 individuals with preserved orbital roofs (8 adults, 1 adolescent and 4 children), CO was diagnosed only for one 6-year-old individual (12038B). Similarly, among 12 individuals with bones of the cranial vault present (9 adults, 1 adolescent and 2 children) probable lesions were visible on only a single cranial vault of a subadult individual (12027).

Ankylosis, a stiffness of the joints that may result from advanced degenerative joint disease or as a fracture complication (Waldron 2009), was present in the skeletons of two individuals. In the first case, the right talus and calcaneus of a male individual (12030C; 45–49* years old) were completely fused (**Figure 2**). The coalition was accompanied by the reduction of both width and length of the talus. Moreover, the distal metaphysis of the right fibula was slightly bent in the posterior direction, while osteoarthritis was observed on its talar articular surface. Besides lumbar spondylosis, degenerative joint disease was observed also on the proximal end of the right ulna and articular processes of the lumbar vertebrae.

The initial phase of ankylosis was documented also in the vertebral column of an adult female (12033B; 40–44 years old). Transverse and intervertebral articular



Figure 4. Possible perimortem trauma on the right parietal bone of a male individual (12047D). Scale bar 1cm.

processes of the lumbar spine were deformed and enlarged by advanced osteoarthritis, being further progressed on the left side. The most evident beginning of fusion was observed between the 5th lumbar vertebra and the sacral bone. Moreover, four medial and distal phalanges of the foot were completely fused. Osteoarthritis was also present in the cervical and thoracic parts of the vertebral column, on the heads of ribs, and right patella, as well as both femoral heads and acetabula.

Furthermore, the skulls of three adult male individuals exhibited different types of injuries. Two crania had signs of sharp force trauma (cf. Love 2019). In the case of the first male individual (12035; 30–35 years old) there were two completely healed parallel injuries on the left parietal bone. One was 33mm long, initiating at the coronal suture and continuing at an angle in the posterior direction. The second trauma was 24.5mm long and situated along the sagittal suture (**Figure 3**). The central parts of both parietal bones were highly porous, which was most probably a result of an inflammatory condition. Furthermore, the fibulae of this individual were asymmetrical, the left bone was about 11 mm shorter and its distal end was slightly deformed. Osteoarthritis was observed in the thoracic spine.

The skull of another adult male individual (12047D) bears evidence of a sharp force trauma without any signs of healing. The injury was present on the right parietal bone and, judging by the size (32mm length, 10mm width) and flat, smooth posterior edge of the lesion, the trauma was most probably aimed from the back, at a high angle (**Figure 4**). Moreover, above lambda there was a region of dense porosity.



Figure 5. Healed trauma on the frontal bone of a male individual (12047A; 40–50 years old).

The skull of the third male (12047A; 40–50 years old) was also injured. A completely healed semicircular fracture (40mm length, 5mm width) was observed on the right side of the frontal bone (**Figure 5**). Another concentric impression, substantially larger than the first lesion (54mm in diameter), and attributed to the blunt force trauma (cf. Kranioti 2015), was present on the left parietal bone (**Figure 6**). A similar, but smaller, injury was also located on the left frontal bone (**Figure 7**). No signs of healing were observed in either of these traumatic lesions. The pattern of fractures suggests that the bone was fresh and elastic during the injury, and therefore the observed fractures may be a result of perimortem trauma (Sauer 1998).

Moreover, in the case of one female (12033C; 25–29 years old) completely healed fractures of both fibulae were observed. Both of them were broken in the middle



Figure 6. Possible perimortem trauma on the left parietal bone of a male individual (12047A; 40–50 years old). Scale bar 1cm.



Figure 7. Possible perimortem trauma on the frontal bone of a male individual (12047A; 40–50 years old).

part of the diaphysis, but the injury of the right bone was situated 2cm further in the distal direction. In both cases, trauma was followed by change in bone geometry and periosteal reaction. Furthermore, osteoarthritis developed in multiple postcranial joints: in the cervical and lumbar spine, sternal manubrium, proximal ends of both fibulae, 1st metatarsal, rib head and foot phalanx. Spondylosis was observed only in the lumbar part of vertebral column.

To conclude, while the frequency of caries, *cribra orbitalia* and porotic hyperostosis in the population of Qareh Tepe was relatively low, traumatic lesions were abundant. A low percentage of stress markers is typical of other Iron Age cemeteries in Iran, but no other site has, to date, presented such a high prevalence of injuries. Only at Molla Kheil, a Parthian site in Mazandaran province, one skeleton with large and healed cranial trauma was found (Sołtysiak et al. 2009). These results suggest that the quality of life of individuals from Qareh Tepe was relatively good, however the degree of inter-personal violence could have been high.

Acknowledgments: Research on human remains from Qareh Tepe was financially supported by the Polish National Science Centre (grants No. 2016/22/M/HS3/00353 and No. 2017/27/N/HS3/01373) and the Institute of Archaeology, University of Tehran. Thanks are due to Pegah Goodarzi for her assistance.

References

- Acsádi G., Nemeskéri J. (1970), *History of human life span and mortality*, Budapest: Akadémiai Kiadó.
- AlQahtani S.J., Hector M.P., Liversidge, H.M. (2010), *Brief communication: The London atlas of human tooth development and eruption*, *American Journal of Physical Anthropology*, 142(3):481-490.
- Brickley M., McKinley J. (eds.) (2004), *Guidelines to the standards for recording human remains*, Reading: BABAO & Institute of Field Archaeologists.
- Brooks S., Suchey J.M. (1990), *Skeletal age determination based on the os pubis: A comparison of the Acsádi-Nemeskéri and Suchey-Brooks methods*, *Journal of Human Evolution* 5:227-238.
- Buckberry J.L., Chamberlain A.T. (2002), *Age estimation from the auricular surface of the ilium: A revised method*, *American Journal of Physical Anthropology* 119:231-239.
- Buikstra J.A., Ubelaker D.H. (eds.) (1994), *Standards for data collection from human skeletal remains*, Fayetteville: Arkansas Archaeological Survey.
- Fejerskov O. (2004), *Changing paradigms in concepts of dental caries: consequences for oral health care*, *Caries Research* 38:182-191.
- Hillson S. (1996), *Dental anthropology*, Cambridge: Cambridge University Press.

- Hillson S. (2001), *Recording dental caries in archaeological human remains*, *International Journal of Osteoarchaeology* 11:249-289.
- Hosseinzadeh J., Sarlak S., Kavosi A., Rafie H., Sołtysiak A. (2018), *Human remains from Sarm, Iran, 2015*, *Bioarchaeology of the Near East* 12:103-106.
- Kranioti E. (2015), *Forensic investigation of cranial injuries due to blunt force trauma: Current best practice*, *Research and Reports in Forensic Medical Science* 5:25-37.
- Love J.C. (2019), *Sharp force trauma analysis in bone and cartilage: A literature review*, *Forensic Science International* 299:119-127.
- McIlvaine B.K. (2015), *Implications of reappraising the iron-deficiency anemia hypothesis*, *International Journal of Osteoarchaeology* 25:997-1000.
- Phenice T.W. (1969), *A newly developed visual method of sexing the os pubis*, *American Journal of Physical Anthropology* 30:297-301.
- Sauer N.J. (1998), *The timing of injuries and manner of death: Distinguishing among antemortem, perimortem and postmortem trauma*, [in:] "Forensic osteology: Advances in the identification of human remains", 2nd edition, K.J. Reichs (ed.), Springfield: Charles C. Thomas, pp. 321-332.
- Scheuer L., Black S., Schaefer M.C. (2010), *Juvenile osteology: A laboratory and field manual*, New York: Academic Press.
- Sołtysiak A., Amirkolaei E., Ghasemi S., Miri M. (2009), *Ghal-e-Kash, Tepe Lafoor & Molla Kheil (Iran), season 2009*, *Bioarchaeology of the Near East* 3:41-47.
- Sołtysiak A., Azizi E., Tawhidi F. (2018), *Human remains from Sanandaj-Zagros, Iran, 2008*, *Bioarchaeology of the Near East* 12:81-83.
- Sołtysiak A., Hosseinzadeh J., Javeri M., Bebel A. (2017), *Human remains from Estark, Iran, 2017*, *Bioarchaeology of the Near East* 11:84-89.
- Steckel R.H., Larsen C.S., Sciulli P.W., Walker P.L. (2011), *The Global History of Health Project. Data collection codebook*, available online.
- Szymczak J., Hosseinzadeh J., Javeri M., Sołtysiak A. (2018), *Human remains from Estark 1, Iran, 2018*, *Bioarchaeology of the Near East* 12:69-75.
- Waldron T. (2009), *Palaeopathology*, Cambridge: Cambridge University Press.
- Walker P.L., Bathurst R.R., Richman R., Gjerdrum T., Andrushko V.A. (2009), *The causes of porotic hyperostosis and cribra orbitalia: A reappraisal of the iron-deficiency-anemia hypothesis*, *American Journal of Physical Anthropology*, 139:109-125.